

## Ka-Band FET Oscillator

ASHOK K. TALWAR, SENIOR MEMBER, IEEE

**Abstract** — The design and performance of GaAs FET oscillators operating near 36 GHz are presented. The oscillators used readily available GaAs FET's and were built in a microstrip circuit configuration. An output power of about +8 dBm was obtained with two devices in a single oscillator.

### I. INTRODUCTION

The purpose of the effort reported here was to build an oscillator operating in the upper *Ka*-band by utilizing widely available FET's and by mounting them in a low-cost circuit configuration. A frequency of 35.9 GHz was targeted to meet a specific military application. The advantages to be gained over other oscillator types, such as those employing Gunn diodes, were lower power dissipation, easy availability of devices with repeatable characteristics, and lower production costs.

This paper discusses characterization of the device used and the circuit employed. The oscillator construction is described and test results obtained on laboratory models are given.

### II. DEVICE CHARACTERIZATION

The NEC NE70000 FET was chosen for this effort because of its extensive usage in the industry, its low cost, and an  $f_{max}$  of greater than 70 GHz. Devices somewhat similar to this are built by several manufacturers.

An equivalent circuit model of the device was developed, based on *S*-parameters available from the manufacturer's data sheet for frequencies up to 18 GHz. Data for a drain to source voltage of 3 V and a drain current of 30 mA were used. The resulting model is shown in Fig. 1. This model was used to calculate *S*-parameters at the frequencies of interest. A similar approach has been taken by Maki *et al.* [1] in their work on a monolithic FET oscillator.

### III. DESCRIPTION OF THE OSCILLATOR CIRCUIT

Several circuit configurations were considered. Based on considerations of realizability as well as electrical parameters, the configuration of Fig. 2 was selected. A somewhat similar circuit has been used by Tseng and Kim [2]. The output (drain) stability circle for the FET with a 0.05-nH inductor connected between the gate and ground is shown in Fig. 3. The region of potential instability is inside the circle. An inductance of 0.05 nH (connected to the drain) falls nearly at the center of the circle. These calculations were done at 36 GHz.

The reflection coefficient ( $\Gamma_{osc}$ ) looking into the circuit of Fig. 2 was calculated as a function of frequency. A plot of its inverse is shown in Fig. 4, along with the inductor values. The 0.07-nH element accounts for the inductance of bond wires needed to connect the source to the output line. It is apparent that a resistive load of around 25  $\Omega$  will cause oscillations in the vicinity

of 36 GHz. This conclusion is based on small-signal calculations. In order to obtain near-maximum power at the desired frequency of 35.9 GHz, an appropriate load was achieved empirically with a dielectric resonator coupled to the 50- $\Omega$  output transmission line.

### IV. CONSTRUCTION

The FET chip is soldered to a carrier at the end of a 50- $\Omega$  microstripline as shown in Fig. 5. The microstrip substrate is 0.01-in-thick Duroid 5880. The source pad is adjacent to the 50- $\Omega$  line. Four bond wires each about 0.014 in long are connected between the source and the output line. The device has two gate and two drain pads. A 0.5-pF ceramic capacitor is mounted adjacent to each of these pads. The capacitors are Dielectric Labs-type D12AOR5B100P. These have a series resonant frequency of about 26 GHz and consequently present some net inductance at 36 GHz. Two wires about 0.01 in long are connected between each gate or drain pad and the adjacent chip capacitor. All bond wires connected to the FET chip are 0.0007-in-diam gold.

The carrier is mounted in a 0.160-in-wide housing. Bias for gate and drain is supplied through 100-pF feed-thru capacitors mounted in the walls of the housing. A 0.002-in-diam, 0.08-in-long wire is used to connect these capacitors with one of the chip capacitors adjacent to a drain or a gate pad. A similar wire is also connected between the microstripline and the ground (housing). The output connector is Omni Spectra SSMA-type 1452-1201-00. A coax to waveguide transition was used to connect the oscillator to the test equipment.

In an effort to increase the output power, oscillators were built with two FET's connected in parallel, as shown in Fig. 6. A repositioning of the resonator was needed to optimize the output power, which increased by about 3 dB. A photograph of such an oscillator is shown in Fig. 7.

### V. TEST RESULTS

Several lab models were built. Some units were also built using the NEC-type NE71000 FET with similar results. With just the 50- $\Omega$  load connected to the circuit, oscillations with about -3-0-dBm output power were observed in the vicinity of 36 GHz. The power output increased to about +5.0 dBm when a dielectric resonator was coupled to the output microstripline. The dielectric material used was Barium Tetratitanate (Trans-Tech-type D-38) with a dielectric constant of 37.

A summary of the data observed on the oscillators is given in Table I. Unit no. 2 employed 0.5-pF MOS capacitors (SDI-type DC-15000-0) instead of the ceramic capacitors. These have a lower parasitic inductance and result in a higher operating frequency.

The dual-transistor oscillators behaved in about the same way as those with a single device except for the power output. They operated with about 0-dBm power output at nearly 36 GHz when the load was 50  $\Omega$ . With a dielectric resonator coupled to the output line, power was in the +7.5-+8.0-dBm range as shown in Table I.

Some of the difference in output frequency among the different models is attributable to variations in the length of bond wires which were not tightly controlled to specific values. Accurate control of bond wire lengths as well as the addition of mechani-

Manuscript received November 3, 1984; revised March 18, 1985.  
The author is with Eaton Corporation, Information Management Systems Division, Micromega, Westlake Village, CA 91362

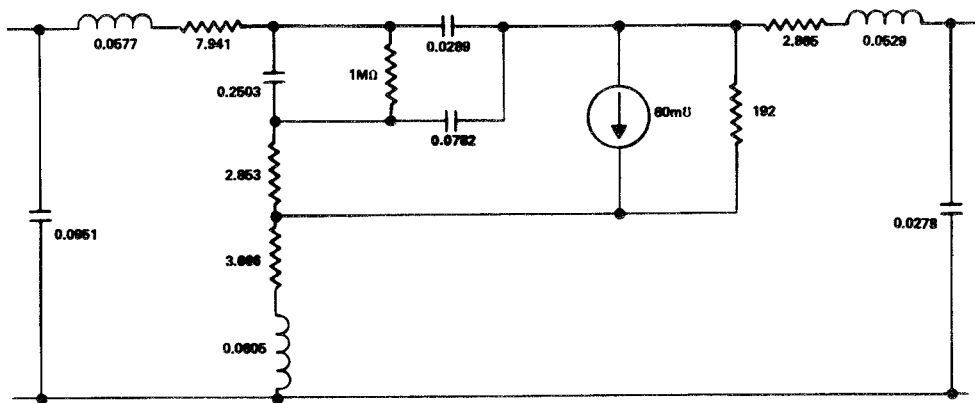


Fig. 1. Equivalent circuit of the FET. Capacitor, inductor, and resistor values are in pF, nH, and ohms.

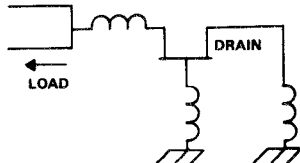


Fig. 2. Oscillator circuit configuration.

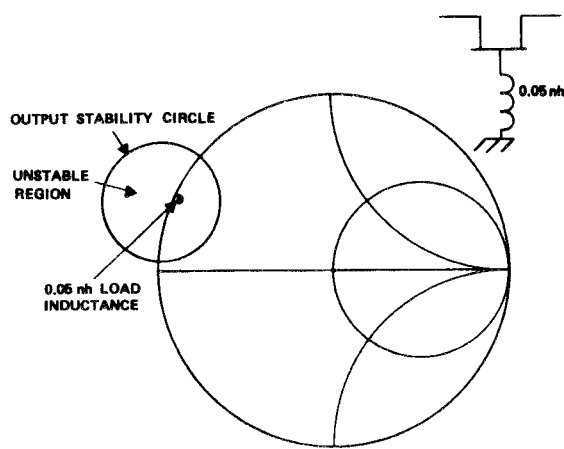


Fig. 3. Output (drain) stability circle.

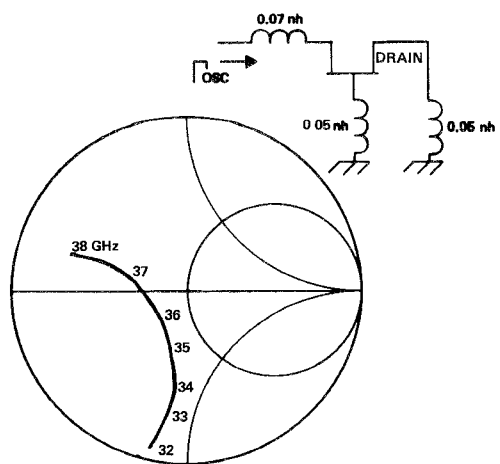


Fig. 4.  $1/\Gamma_{\text{osc}}$  as a function of frequency.

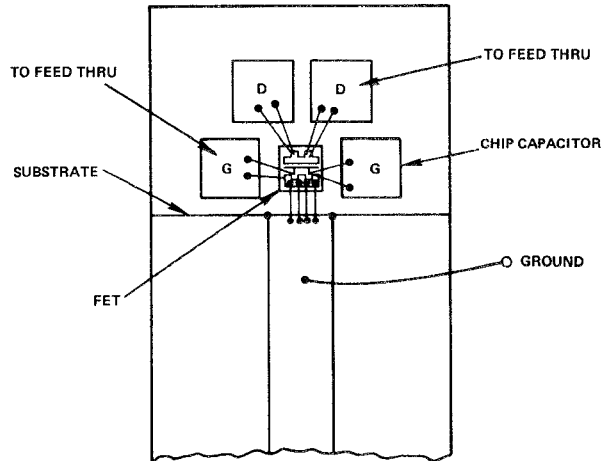


Fig. 5. FET oscillator layout.

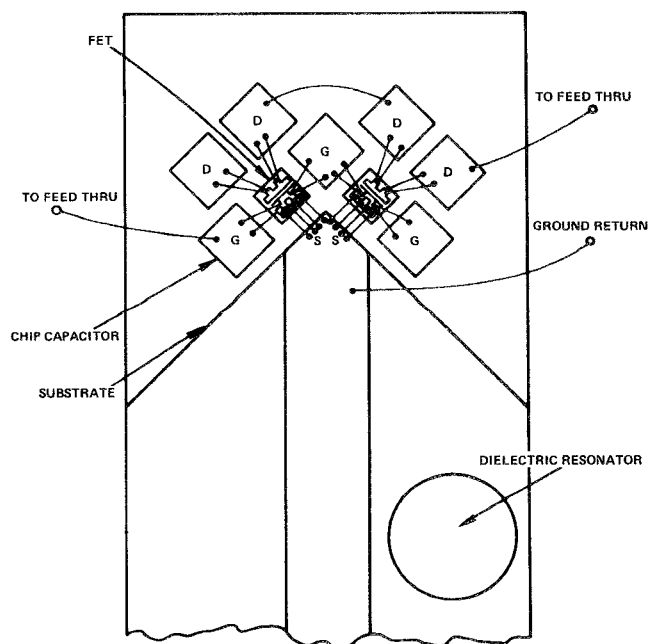


Fig. 6. Dual FET oscillator layout.

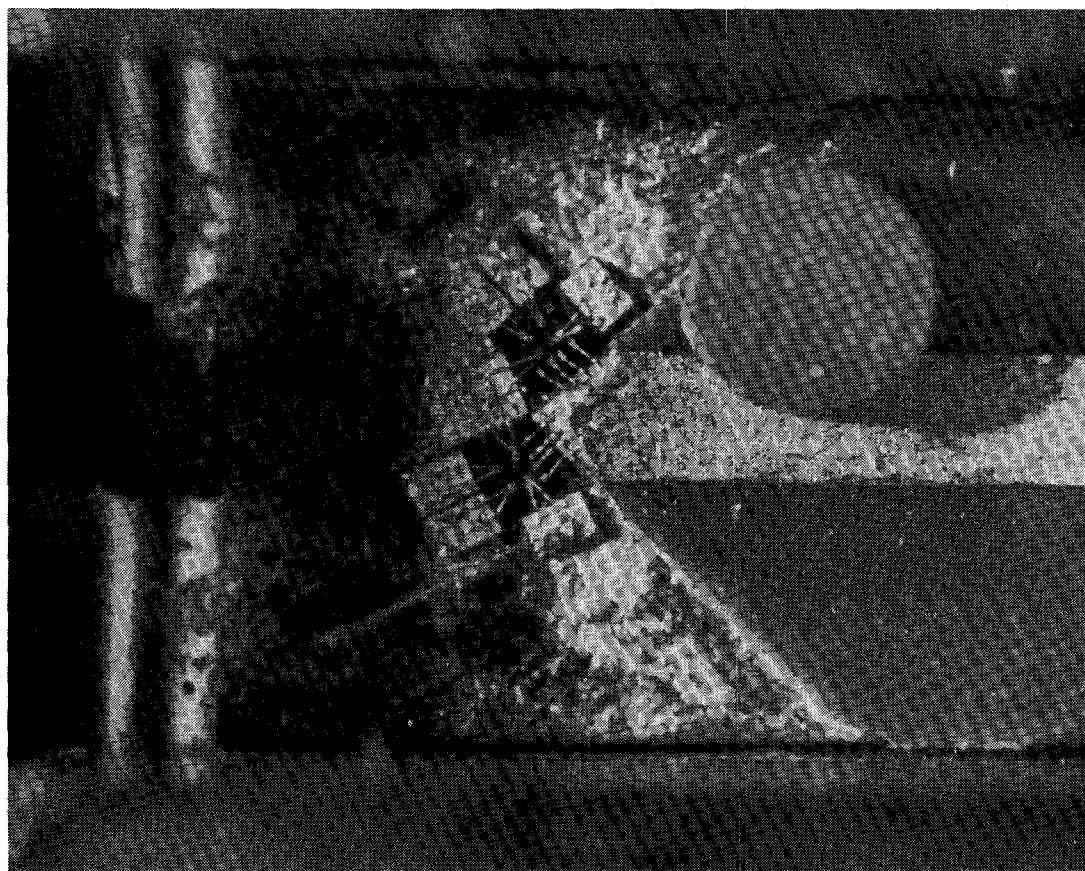


Fig. 7. Dual FET oscillator (S. no. 4).

TABLE I  
FET OSCILLATOR DATA

S. No.	Device	No. of Devices	Frequency GHz	Power dBm	Drain Current mA
1	NE70000	1	36.4	5.0	38
2	NE71000	1	39.9	0.0	35
3	NE70000	2	36.6	7.5	81
4	NE70000	2	35.8	7.9	59
5	NE71000	2	35.3	8.0	42

The drain to source voltage was 4 V in all cases.

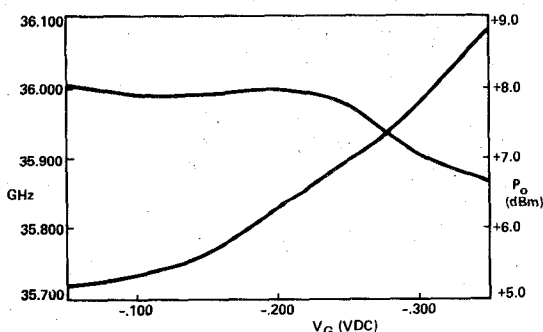


Fig. 8. Power and frequency as a function of gate voltage for S. no. 4.

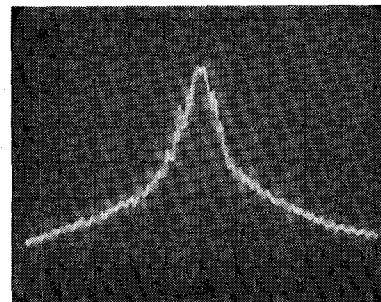


Fig. 9. Output spectrum of an FET oscillator stabilized by a dielectric resonator. Res. BW = 30 KHz. Hor. Div = 100 KHz. Vert. Div = 10 dB.

cal tuning of frequency will be necessary in any production program. Preliminary tests with a tuning screw mounted above the dielectric resonator gave approximately 150 MHz of frequency change within a 1-dB power output window.

The frequency and power shown in the table are for arbitrary values of gate voltage upon which they are dependent. A plot of frequency and power output as a function of gate voltage for S. no. 4 is given in Fig. 8. These curves are typical and show that electronic control of frequency is possible without the addition of a varactor diode to the circuit.

Stability of frequency over temperature was examined. Over a temperature range of  $-40^\circ$  to  $+80^\circ$ C, a total drift of about 40 MHz was observed.

Even with the oscillator stabilized with a dielectric resonator, the spectrum of the output was quite noisy, as shown in Fig. 9. In order to improve the spectral quality, as well as frequency stabil-

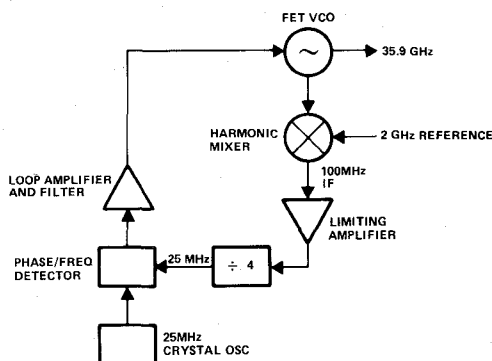


Fig. 10. Functional diagram of the phase-locked VCO.

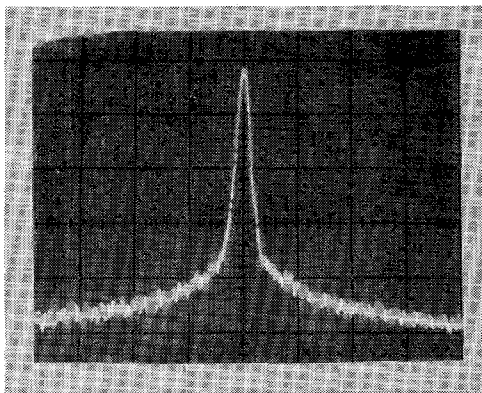


Fig. 11. Output spectrum of an FET oscillator, phase locked to a crystal oscillator. Res. BW = 1 KHz. Hor. Div = 10 KHz. Vert. Div = 10 dB.

ity, it was decided to phase lock one of the oscillators, S. no. 4 in Table I, to a crystal-controlled signal. The oscillator power sample was taken with a coaxial probe mounted on the cover of the VCO housing. A harmonic mixer [3] driven by a stable 2-GHz LO was used to obtain an IF frequency of 100 MHz, the FET oscillator frequency being 35.9 GHz. This IF was locked to a crystal oscillator with the help of a phase-locked loop, as shown in Fig. 10. The resulting spectrum as observed on a spectrum analyzer is shown in Fig. 11.

## VI. CONCLUSION

Ka-band oscillators employing widely available GaAs FET's have been demonstrated. These offer advantages of lower power consumption and potentially lower cost in comparison with Gunn oscillators.

## ACKNOWLEDGMENT

The author thanks R. B. Steinkolk for helpful discussions and G. K. Behringer for running the tests.

## REFERENCES

- [1] D. W. Maki, J. M. Schellenberg, H. Yamasaki, and L. C. T. Liu, "A 69 GHz monolithic FET oscillator," in *IEEE 1984 Microwave and Millimeter-Wave Monolithic Circuits Symp. Dig.*, May 1984, pp. 62-66.
- [2] H. Q. Tserng and B. Kim, "High efficiency Q-band GaAs FET oscillators," *Electron. Lett.*, vol. 20, no. 7, pp. 297-298, Mar. 1984.
- [3] T. Mazilu and A. K. Talwar, "A harmonic mixer for the 20-40-GHz range," *IEEE Trans. Microwave Theory Tech.*, vol. MTT-30, pp. 106-107, Jan. 1982.

## Integral Transforms Useful for the Accelerated Summation of Periodic, Free-Space Green's Functions

R. LAMPE, P. KLOCK, SENIOR MEMBER, IEEE,  
AND P. MAYES, FELLOW, IEEE

**Abstract** — The Poisson summation formulas for two- and three-dimensional, periodic, free-space Green's functions of the Helmholtz and Laplace equations are cataloged in this paper. It is shown how these formulas can be applied for the efficient, approximate summation of series which arise in the computation of fields due to an infinite array of charge or current sources. The technique for approximating the summation of the series is valid for all arguments of a Green's function, even those which correspond to the region near a source singularity.

## I. INTRODUCTION

The computation of fields due to periodic sources can arise in the application of image theory when multiple ground planes are present. When the ground planes are closely spaced, the contribution to the field due to direct summation of the image sources is impractical due to very slow convergence. Hence, the image technique has been of limited usefulness in solving problems such as those involving striplines or cavities.

The Poisson summation formula [1] can sometimes be used to convert a slowly converging series into a rapidly converging one by allowing the series to be summed in the Fourier transform domain. To date, the Poisson summation formula has, when applied to periodic sources, been primarily applied to cases of determining fields at a distance from a source region. If the terms of a spatial domain series represent sampling of a function which is singular or nearly singular, such as the field near a source, the summation in the transform domain could be as slowly convergent as that in the spatial domain. Typically, the determination of a charge or current distribution for an element in a periodic array involves the evaluation of the field near a source singularity precluding useful application of the Poisson summation formula.

## II. SERIES ACCELERATION TECHNIQUE

A technique has been described for accelerating the summation of periodic, free-space Green's functions which circumvents the difficulty of slow convergence near a source singularity [2]. In its most basic form, this technique begins with two periodic functions: one for which a sum is required, and another which is asymptotically equal to the first but is smooth everywhere. These two functions will be defined as

$$\sum_{n=-\infty}^{\infty} f(n) \text{ and } \sum_{n=-\infty}^{\infty} g(n)$$

respectively. The equation which represents this technique is derived by combining Kummer's transformation [3] and the Poisson summation formula to obtain the following approximation:

$$\sum_{n=-\infty}^{\infty} f(n) \approx \sum_{n=-K}^{K} [f(n) - g(n)] + \sum_{n=-\infty}^{\infty} G(2\pi n) \quad (1)$$

Manuscript received September 14, 1983; revised March 18, 1985. This work was supported in part by RCA, Government Systems Division, Missile and Surface Radar, Moorestown, NJ.

R. Lampe is with RCA, Missile and Surface Radar, Moorestown, NJ 08057. P. Klock and P. Mayes are with the Department of Electrical Engineering, University of Illinois, Urbana, Illinois 61801.